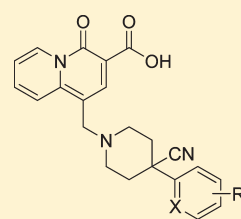


Discovery of a Selective Allosteric M₁ Receptor Modulator with Suitable Development Properties Based on a Quinolizidinone Carboxylic Acid Scaffold

Scott D. Kuduk,^{*,†} Ronald K. Chang,[†] Christina N. Di Marco,[†] Daniel R. Pitts,[†] Thomas J. Greshock,[†] Lei Ma,[‡] Marion Wittmann,[‡] Matthew A. Seager,[‡] Kenneth A. Koeplinger,[§] Charles D. Thompson,[§] George D. Hartman,[†] Mark T. Bilodeau,[†] and William J. Ray[‡]

Departments of [†]Medicinal Chemistry, [‡]Alzheimer's Research, and [§]Drug Metabolism, Merck Research Laboratories, Sumneytown Pike, P.O. Box 4, West Point, Pennsylvania 19486, United States

ABSTRACT: One approach to ameliorate the cognitive decline in Alzheimer's disease (AD) has been to restore neuronal signaling from the basal forebrain cholinergic system via the activation of the M₁ muscarinic receptor. A number of nonselective M₁ muscarinic agonists have previously shown positive effects on cognitive behaviors in AD patients, but were limited due to cholinergic adverse events thought to be mediated by the activation of the M₂ to M₅ subtypes. One strategy to confer selectivity for M₁ is the identification of positive allosteric modulators, which would target an allosteric site on the M₁ receptor rather than the highly conserved orthosteric acetylcholine binding site. Quinoline carboxylic acids have been previously identified as highly selective M₁ positive allosteric modulators with good pharmacokinetic and in vivo properties. Herein is described the optimization of a novel quinolizidinone carboxylic acid scaffold with 4-cyanopiperidines being a key discovery in terms of enhanced activity. In particular, modulator **4i** gave high plasma free fractions, enhanced central nervous system (CNS) exposure, was efficacious in a rodent in vivo model of cognition, and afforded good physicochemical properties suitable for further preclinical evaluation.



INTRODUCTION

One of the consequences of Alzheimer's disease (AD) is the progressive degeneration of the neurons of the basal forebrain cholinergic system, which manifests in the form of profound cognitive deficits.¹ The front line of treatment for AD symptoms is acetylcholinesterase inhibitors which act by limiting the degradation of synaptic acetylcholine (ACh) levels to activate cholinergic receptors. While these agents have established efficacy for the treatment of AD symptoms, the magnitude and duration of the effects are limited, partly owing to the general activation of numerous receptor subtypes.

ACh activates both nicotinic (ligand-gated ion channels) and muscarinic (metabotropic) receptors, which belong to the class A family of G protein coupled receptors (GPCRs). The muscarinic acetylcholine receptors play critical roles in the regulation of higher cognitive function. There are five receptor subtypes in the muscarinic family (classified M₁ to M₅),^{2,3} of which the M₁ receptor is most highly expressed in areas that are critically involved in memory formation such as the cortex and hippocampus, and are affected prominently in AD. Additionally, M₁ knockout mice have demonstrated deficits in the prefrontal cortex and hippocampus dependent memory tasks. Consequently, M₁ has been widely viewed as the subtype most likely affecting cognitive and memory effects in this region of the brain.⁴

As a result, a number of nonselective or partially selective M₁ agonists such as xanomeline have been evaluated clinically for the treatment of AD. Compounds indeed progressed into clinical trials where they were intended to enhance cognitive

performance in AD patients.^{5,6} However, adverse events such as gastrointestinal distress, salivation, sweating, and emesis have prevented their clinical utility. It has been thought that these events are mediated by the activation of other peripheral muscarinic receptors and that an M₁ selective compound would have improved tolerability.

It has proven difficult to identify highly subtype selective agonists for the M₁ receptor due to the high sequence homology of the orthosteric acetylcholine binding site. One alternate strategy to address this is to target allosteric binding sites on the M₁ receptor that should be less highly conserved and provide preference for M₁ over the M₂–M₅ subtypes.⁷ Accordingly, M₁ selective activators in the form of allosteric agonists such as AC-42⁸ and TBPB,⁹ or positive allosteric modulators¹⁰ should provide the high selectivity over their orthosteric comparators.

In this regard, the discovery of quinolone carboxylic acid **1**^{11,12} from a high throughput screen (HTS) has been reported as a highly M₁ selective positive allosteric modulator (Figure 1). Compound **1** presented modest M₁ receptor functional activity and brain penetration, high plasma protein binding, and low solubility in a neutral form. As a result, high plasma levels were required for in vivo efficacy. A thorough SAR study was conducted on the methoxybenzyl group leading to biaryl and fused heterocyclic analogues,^{13–16} as well as the identification of alternatives to the phenyl A-ring of the quinolone ring system (Figure 1).^{13,14} While these modifications maintained the high

Received: April 4, 2011

Published: June 17, 2011

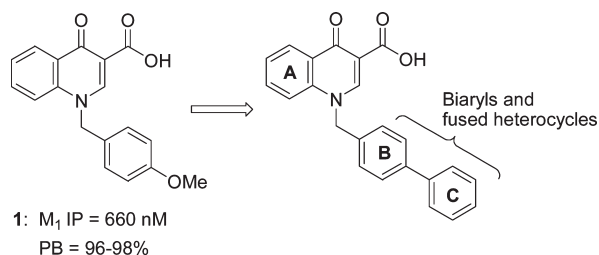


Figure 1. HTS lead.

level of selectivity for the M_1 receptor subtype with some variable improvements in brain exposure/in vivo efficacy, minimal advances were made in terms of optimal pharmacological and physicochemical profiles.

In an attempt to improve upon the physical properties of 1, alternative ring systems for the quinolone were examined. One such construct is represented in the form of the quinolizidinone nucleus in compound 2 (Figure 2).¹⁵ It was found that the quinolizidinone ring system was a molecular homologue of the quinolone providing compounds with similar or enhanced M_1 functional activity. Moreover, this strategy allowed for the incorporation of a basic amine at the benzylic position of 2 in the form of a 4-cyanophenyl piperazine, which could not be achieved in the quinolone context. Most importantly, this latter modification provided compounds that were not subject to efflux by the CNS efflux transporter *P*-glycoprotein (*P*-gp), with increased free fraction, solubility, and CNS exposure. Previous attempts at incorporation of basic amines in the quinolone carboxylic acid series as shown by the generic structure in Figure 2 led to compounds that were substrates for *P*-gp mediated efflux.

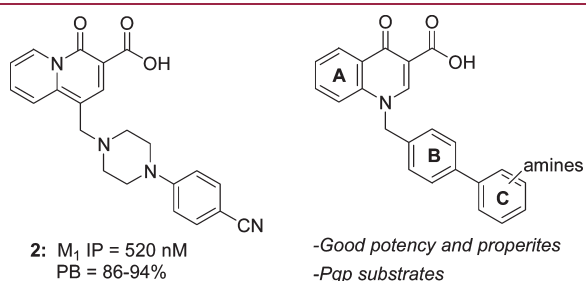
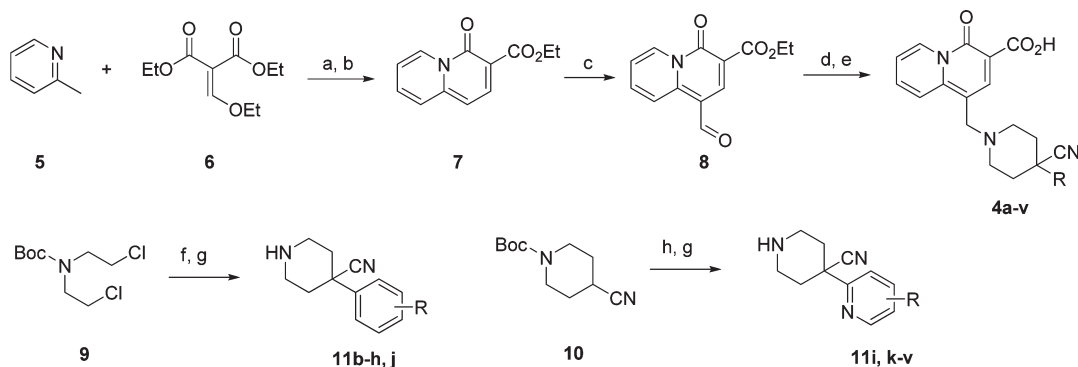


Figure 2. Quinolizidinone lead and quinolone amine strategy.

Scheme 1^a

^a (a) LDA, THF, -80 to -20 °C. (b) *o*-Xylene, reflux. (c) POCl_3 , DMF, 0 to 20 °C. (d) 11a-v, $\text{NaBH}(\text{OAc})_3$, DCE, AcOH, molecular sieves. (e) NaOH, THF, EtOH, 50 °C. (f) phenylacetonitrile, NaH, DMSO. (g) HCl, EtOAc, 0 °C. (h) LiHMDS, halo-pyridine, THF, -78 °C.

Optimization attempts focused on the piperazine region of 2. In general, the SAR for this chemical space was generally flat, a common observation in allosteric modulator lead optimization,¹⁰ with limited improvements in terms of functional activity. Piperidines were also investigated as replacements for the piperazine, but again flat SAR was observed, with no significant in vivo activity of note for analogues that were examined.¹⁶

In this article, we describe a major exception to this flat SAR profile in the form of quinolizidinone 4a bearing a cyano group at the 4-position of the piperidine. Modulator 4a was found to have ~ 9 -fold increase in functional activity (M_1 IP = 151 nM) relative to that of unsubstituted piperidine 3 (Figure 3). Herein, we describe efforts to optimize 4a and identify a brain penetrant, orally bioavailable, selective M_1 allosteric modulator leading to the discovery of such a quinolizidinone analogue with suitable development properties for potential investigation as a clinical compound.

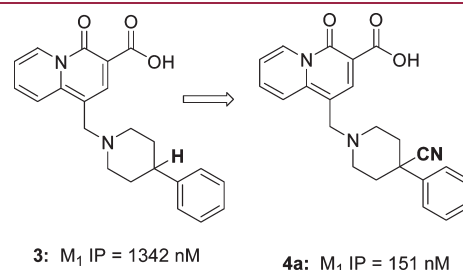


Figure 3. Insertion of cyano.

CHEMISTRY

The chemical route used to access target molecules examined in this article is shown in Scheme 1.¹⁷ Lithiation of 2-picoline 5 with *n*-butyllithium was followed by addition of ethoxymethylene diethylmalonate 6 and subsequent cyclization in refluxing *ortho*-xylene to provide quinolizidinone ethyl ester 7. Vilsmeier formylation was effectively carried out at the 1-position to afford requisite aldehyde 8.¹⁸ Reductive amination of 8 with the appropriate amines was conducted using sodium triacetoxy borohydride in dichloroethane followed by saponification of the ethyl ester to provide target quinolizidinone carboxylic acids 4a–v. The 4-aryl-4-cyano piperidines employed in this study were prepared via bis-alkylation of 9 with an appropriate aryl acetonitrile. For the synthesis of 4-pyridyl-4-cyano piperidines, a

recently developed, highly efficient S_NAr reaction was utilized between **10** and the appropriate halo-pyridines.¹⁹

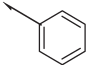
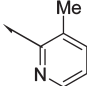
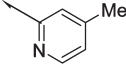
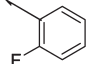
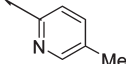
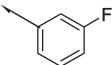
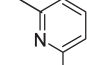
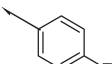
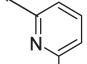
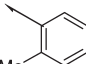
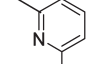
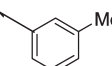
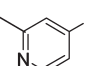
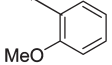
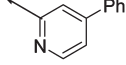
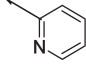
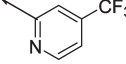
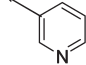
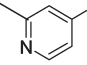
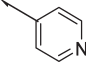
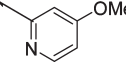
BIOLOGICAL RESULTS AND DISCUSSION

The structure–activity relationship (SAR) data for potency and protein binding of select analogues is shown in Table 1. Compound potencies were determined in the presence of an EC_{20} concentration of acetylcholine at human M_1 expressing Chinese hamster ovary (CHO) cells using calcium mobilization readout on a fluorometric imaging plate reader (FLIPR₃₈₄). Plasma protein binding was determined using the equilibrium dialysis method in the presence of rat or human serum. Studies of

P-gp mediated directional transport were performed in LLC-PK1 cells expressing genes for human P-gp (multidrug resistance, MDR1), and the ratio of transport from basolateral to apical (B to A) direction to the ratio of transport from apical to basolateral (A to B) direction was measured. Full details for the previous experiments are described in Experimental Procedures.

In addition to the aforementioned M_1 functional activity of phenyl analogue **4a** (M_1 IP = 151 nM), ~10% free fraction was also observed in rat and human plasma protein. The phenyl group was critical as the unsubstituted 4-cyano piperidine **4b** lost ~50-fold in potency. A fluorine at the ortho position (**4c**) enhanced potency, with a small increase in protein binding, while little or no benefit was seen with the meta (**4d**) or para (**4e**)

Table 1. Quinolizidinone SAR

Cmpd	R	M_1 Pot IP (nM) ^a	Rat PB	Human PB	Cmpd	R	M_1 Pot IP (nM) ^a	Rat PB	Human PB
4a		151	86.5	89.9	4l		1939	-	-
4b	H	7649	-	-	4m		44	53.3	76.5
4c		81	89.8	94.5	4n		204	65.2	82.5
4d		562	-	-	4o		148	75.1	84.2
4e		194	-	-	4p		100	94.3	98.8
4f		68	94.9	96.2	4q		133	78.2	92.9
4g		88	94.1	95.2	4r		84	72.8	86.6
4h		164	-	-	4s		659	-	-
4i		135	68.2	70.9	4t		2720	-	-
4j		363	49.1	63.9	4u		244	-	-
4k		938	-	-	4v		224	51.5	78.3

^a Values represent the numerical average of at least two experiments. IP, inflection point; PB, protein binding. Interassay variability was $\pm 30\%$ (IP, nM), unless otherwise noted.

variants. The *o*-tolyl analogue **4f** was the most potent in the series with an M_1 IP = 68 nM, with an ~5% free fraction, although the meta-isomer was also well tolerated. Electron donating groups such as methoxy **4h** conferred little benefit.

Incorporation of a nitrogen in the form of a pyridine (**4i–k**) in lieu of the phenyl was examined as an avenue to further reduce plasma protein binding. The 2-pyridyl analogue **4i** was similarly potent to phenyl analogue **4a**, with the desired marked reduction in plasma protein binding (68–71%). The 3- and 4-pyridyl isomers **4j–k** lost substantial M_1 functional activity.

Accordingly, a wide range of analogues of **4i** that possessed substitution on the pyridine was investigated. A methyl scan was conducted (**4l–o**) in which all positions except the 6-methyl (**4l**, M_1 IP = 1939 nM) were neutral or led to a potency increase. The 3- and 5-positions were chosen for additional SAR due to the combination of potency and free fraction observed with the methyl analogues (**4m**, **4o**), and select compounds are detailed in Table 1. With respect to the 3-position, thiomethyl and chloro substituents moderately enhanced functional activity relative to methyl, but did have substantial increases in protein binding. Analogues at the 5-position (**4r–v**) gave more variable results. In general, larger groups such as phenyl **4s** (M_1 IP = 659 nM) and trifluoromethyl **4t** (M_1 IP = 2720 nM) showed reduced activity relative to that of heteroatom attachment such as fluoro **4u** (M_1 IP = 244 nM) and methoxy **4v** (M_1 IP = 224 nM). The best compounds were the small aliphatic groups in the form of the aforementioned **4m** and ethyl **4r** (M_1 IP = 84 nM).

Having identified a number of 4-substituted-4-cyanopiperidines from Table 1, the brain exposure properties for select compounds were examined. The efflux transporter P-gp is considered the predominant mechanism for efflux of a number of xenobiotic substances from the CNS at the blood–brain barrier. For that reason, compounds were first evaluated for their permeability properties (P_{app}) and susceptibility as P-gp substrates in order to further assess their CNS exposure potential. As can be seen from Table 2, all of the compounds possessed good passive permeability ($P_{app} > 15$) and were not substrates for human (MDR1), although **4a** and **4m** were substrates for the rat (MDR1a) variant.

CNS penetration was measured by oral dosing of rats at 10 mpk, and bioanalysis of plasma, brain, and CSF levels was taken at two hours. Phenyl analogue **4a** provided good CSF and brain to plasma ratios, but gave low plasma levels. It is worth noting that **4a** is a substrate for rat P-gp, and this could be limiting the CNS exposure. However, similar results were obtained with the more potent tolyl analogue **4f**, which was not a rat P-gp substrate. While 2-pyridine **4i** had slightly reduced permeability compared to that of **4a** and **4f**, it gave substantially higher plasma levels and CSF levels. Interestingly, the isomeric 3-pyridyl analogue **4j** had the best permeability and highest free fraction

among the group, but exhibited vastly inferior CSF and total brain levels⁵⁰ despite higher plasma levels than those of **4i**. Lipophilicity could be a factor in the CNS exposure as **4i** is more lipophilic ($\log P = 0.15$), than **4j** ($\log P = -0.4$). Last, addition of a 5-methyl on the 2-pyridyl nucleus (**4m**) provided an approximate 2-fold increase in plasma levels relative to that of **4i**, although the CSF and brain to plasma ratios were slightly reduced.

On the basis of their potency, free fraction, and brain exposure profiles, compounds **4i** and **4m** were chosen for additional pharmacokinetic characterization (Table 3). The unsubstituted pyridine **4i** exhibited good oral bioavailability in rats (68%) with a relatively low clearance and a half-life of 1.7 h. Similar bioavailability was observed in dogs (62%), with a longer half-life. The 4-methyl pyridine **4m** had relatively lower bioavailability in both rats (24%) and dogs (47%), with slightly higher clearances than those of **4i**.

The pharmacokinetics of **4i** was also measured in rhesus monkeys and was found to possess good bioavailability (55%) with a 3.6 h half-life and clearance of 17 mL/min/kg. Thus, compound **4i** exhibits good pharmacokinetic properties across three different species with the potential for good human oral bioavailability. Accordingly, **4i** was selected for further in depth characterization.

Table 3. Rat and Dog Pharmacokinetics for Select Compounds

cmpd	rat PK ^a			dog PK ^b		
	F (%)	$t_{1/2}$ (h)	Cl mL/min/kg	F (%)	$t_{1/2}$ (h)	Cl mL/min/kg
4i	68	1.7	13.5	62	4.4	7.4
4m	24	1.9	17.7	47	3.9	10.1

^aRat ($n = 2$). Oral dose, 3 mg/kg; IV dose = 1 mg/kg. Interanimal variability was less than 20% for all values. ^bDog ($n = 2$). Oral dose, 3 mg/kg; IV dose = 1 mg/kg. Interanimal variability was less than 20% for all values.

Metabolism studies conducted with nicotinamide adenine dinucleotide phosphate (NADPH)-fortified hepatic microsomes from rats, dogs, monkeys, and humans revealed no detectable oxidative metabolism of modulator **4i**. In hepatocytes, the only metabolic pathway observed was direct conjugation of the carboxylic acid resulting in acyl glucuronide **12** (Figure 4). This was the sole metabolite observed in *in vitro* incubations of **4i** with hepatic, intestinal, and renal microsomes in the presence of uridine diphosphate α -D-glucuronic acid (UDPGA), which is a cofactor for uridine glucuronosyltransferase (UGT) activity. Rates of formation of **12** were higher in intestinal and renal microsomal incubations than hepatic microsomal incubations suggesting the potential for extrahepatic glucuronidation of **4i**. A study carried out after oral administration of [³H]**4i** to portal

Table 2. Permeability, P-gp, and Bioanalysis of Plasma, Brain, and CSF Levels in Rat for Selected Compounds

cmpd	P_{app} ^a	MDR1 ^b	MDR1a ^b	plasma concn (nM) ^c	brain concn (nM) ^c	CSF concn (nM) ^c	brain/plasma	CSF/ U_{plasma} ^d
4a	27	1.2	3.5	321	127	8	0.39	0.25
4f	24	1.0	2.1	234	114	16	0.48	0.5
4i	18	0.5	1.4	1482	306	135	0.23	0.3
4j	39	0.9	1.1	1723	0	40	0	<0.1
4m	27	1.2	3.2	3070	233	180	0.07	0.25

^aPassive permeability (10^{-6} cm/s). ^bMDR1 directional transport ratio (B to A)/(A to B). Values represent the average of three experiments, and interassay variability was $\pm 20\%$. ^cSprague–Dawley rats. Oral dose was 10 mg/kg in 90% PEG 400, and interanimal variability was less than 20% for all values. ^dDetermined using rat plasma protein binding from Table 1.

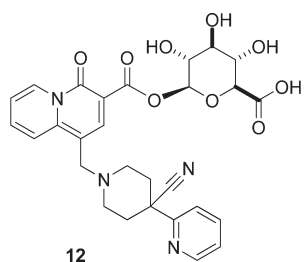


Figure 4. Major metabolite.

vein cannulated (PVC) dogs confirmed a high level ($\sim 50\%$) of presystemic GI glucuronidation as contrasted with a low liver extraction ratio (E_h). Thus, while oral bioavailability was good ($>50\%$) in preclinical species, **4i** exhibits the potential for substantial first pass GI presystemic metabolism.

Quinolizidinone **4i** was evaluated for the ability to sensitize the response to varying doses of acetylcholine in the presence of a fixed concentration of a potentiator. As can be seen from Figure 5, increasing concentrations of the potentiator led to the expected left-ward shift in the acetylcholine dose–response curve. For example, in the presence of $0.1 \mu\text{M}$ of the potentiator, a left-shift of 3-fold was observed, and at $1 \mu\text{M}$, it was 146-fold verifying that **4i** is a potent positive allosteric modulator of the human M_1 receptor. It should be noted that some degree of agonism (i.e., activity of the potentiator in the absence of an ACh response) was observed at $10 \mu\text{M}$ concentration.

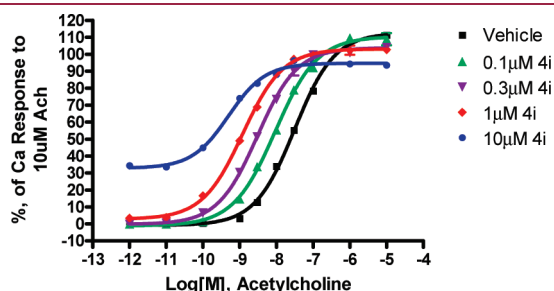


Figure 5. Fold potentiation.

The selectivity for quinolizidinone **4i** in cells expressing human M_2 – M_4 receptors was also examined. Consistent with previous observations from quinolone or quinolizidinone carboxylic acid derived allosteric modulators, no potentiation or agonism of cells expressing M_2 – M_4 receptor subtypes was observed highlighting the selectivity of **4i** for the M_1 . It has been previously reported that quinolizidinone **2** exhibited modest functional blockade of the hERG potassium channel ($IC_{50} = 7.4 \mu\text{M}$), but modulation of the amine basicity in the form of the 4-(2-pyridyl)-4-cyano piperidine in **4i** removed this potential liability ($IC_{50} > 30 \mu\text{M}$). In addition, modulator **4i** possessed M_1 potentiation similar to that of human receptor at rat (M_1 IP = 89 nM), mouse (M_1 IP = 69 nM), dog (M_1 IP = 100 nM), and rhesus (M_1 IP = 49 nM) receptors. Last, **4i** was found to have an exceptionally clean ancillary pharmacology profile with no activity up to $30 \mu\text{M}$ in a screen of 140 targets (Panlabs).

To evaluate in vivo activity, potentiator **4i** was tested in a mouse contextual fear conditioning model of episodic memory, a task that requires the hippocampus, where the M_1 receptor is densely expressed (Figure 6).²¹ In this experiment, the

nonselective muscarinic antagonist scopolamine was administered to block the formation of the association of a novel environment with an aversive stimulus (a foot shock). Quinolizidinone **4i** was codosed at 1, 3, 10, and 30 mpk (i.p.) with scopolamine on the training day and produced no baseline (training day) effects. Mice codosed with **4i** on the training day showed a reversal of scopolamine deficits in a dose dependent manner in terms of freezing behavior compared to that of vehicle treated animals on the test day (24 h). Statistically significant effects were noted at 10 and 30 mpk corresponding to $3 \mu\text{M}$ plasma levels at the 10 mpk dose. By way of comparison, quinolone **1** required $\sim 33 \mu\text{M}$, and quinolizidine **2** $\sim 7.4 \mu\text{M}$, for the reversal of scopolamine deficit in this model.

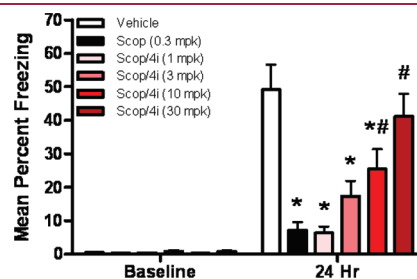


Figure 6. CFC assay results.

CONCLUSIONS

We have identified 4-(2-pyridyl)-4-cyano piperidine derived quinolizidinone carboxylic acid **4i** as a potent and selective M_1 positive allosteric modulator with an exceptionally clean ancillary pharmacological profile. Quinolizidinone **4i** exhibited good pharmacokinetic and CNS exposure properties, and achieved in vivo efficacy in a mouse model of episodic memory at the lowest plasma concentration of any quinolone or quinolizidinone we have examined. On the basis of these properties and the potential for good human pharmacokinetics, **4i** was selected for further evaluation as a potential candidate for clinical development for the treatment of cognitive dysfunction in patients with AD.

EXPERIMENTAL PROCEDURES

General. All commercially available chemicals and solvents were used without further purification. Automated flash chromatography was performed on ISCO CombiFlash with peak detection at 254 nm. Reverse phase purification was accomplished using a Gilson 215 liquid handler equipped with a YMC Pack Pro C18 column ($150 \times 20 \text{ mm}$ I. D., $5\text{--}5 \mu\text{m}$). Peak collection was triggered by UV detection at 214 or 254 nm. ^1H (400 MHz) NMR spectra were recorded on a Varian VXR 400 spectrometer unless otherwise noted. The chemical shifts are reported in δ (ppm) using the δ 0.00 signal of Me_4Si as an internal standard. High-resolution MS data were obtained on Bruker Daltonics FTICR/MS. High-resolution mass spectral analysis was performed on a Bruker-daltonics BioApex 3T mass spectrometer. HPLC spectra were recorded on a Hewlett-Packard 1100 with a CombiScreen Pro C-18 column. The purity of compounds was assessed to be $>95\%$ by analytical HPLC: (i) system 1, linear gradient over 10 min of $\text{CH}_3\text{CN}/0.1\% \text{ TFA}$ and $\text{H}_2\text{O}/0.1\% \text{ TFA}$ 10:90 to 95:5, and 2 min at 95:5; flow rate, 1.0 mL/min ; detection at 215 and 254 nm (YMC-Pack Pro C18, $50 \times 4.6 \text{ mm}$ column). (ii) Linear gradient over 3.5 min of $\text{CH}_3\text{CN}/0.1\% \text{ TFA}$ and $\text{H}_2\text{O}/0.1\% \text{ TFA}$ 5:95 to 95:5; flow rate, 1.5 mL/min ; detection at 215 nm (YMC-Pack Pro C18, $50 \times 4.6 \text{ mm}$ column).

All animal studies described herein were approved by Merck Research Laboratories Institutional Animal Care and Use Committee.

Ethyl 4-Oxo-4H-quinolizine-3-carboxylate (7). To a heat-dried flask under N₂ was added a solution of diisopropylamine (19.1 mL, 0.134 mmol) in THF (1.0 M, 400 mL). The mixture was cooled to −50 °C, and a solution of *n*-butyllithium in hexanes (2.5 M, 53.7 mL, 0.134 mol) was added. After 30 min, the reaction was cooled to −78 °C, and a solution of 2-picoline (10.0 g, 0.107 mol) in THF (0.8 M, 80 mL) was slowly added, keeping the temperature of the reaction below −60 °C. After 30 min, a solution of diethyl ethoxymethylenemalonate (24.5 mL, 0.121 mol) in THF (1.8 M, 67 mL) was slowly added, keeping the temperature of the reaction below −60 °C. The mixture was slowly warmed to −20 °C over 2 h, then poured into water, and extracted 3 times with dichloromethane. The combined organic fractions were concentrated in vacuo, and the residue was dissolved in xylenes (84 mL). The mixture was heated to reflux for 16 h, cooled to room temperature, and filtered. The filtrate was concentrated in vacuo, and the residue was triturated overnight with diethyl ether. The solid was collected via filtration to provide 7 (19.2 g, 82.0%) as an orange brown solid. ¹H NMR (400 MHz, CDCl₃) δ 1.43 (t, *J* = 7.1 Hz, 3H), 4.43 (q, *J* = 7.1 Hz, 2H), 6.66 (d, *J* = 8.5 Hz, 1H), 7.18–7.21 (m, 1H), 7.57–7.63 (m, 2H), 8.41 (d, *J* = 8.6 Hz, 1H), 9.41 (d, *J* = 7.1 Hz, 1H). MS *m/z* = 218.3 (MH⁺).

Ethyl 1-Formyl-4-oxo-4H-quinolizine-3-carboxylate (8). To a solution of compound 7 (10.4 g, 47.9 mmol) dissolved in DMF (2.14 M, 22.4 mL) was added dropwise phosphorus oxytrichloride (11.2 mL, 0.120 mol). After 1 h, the mixture was poured into water and extracted 3 times with dichloromethane. The combined organic fractions were dried over sodium sulfate, filtered, and concentrated in vacuo. The residue was subjected to silica gel chromatography (0–2% methanol in dichloromethane) to provide 8 (4.02 g, 33.9%) as a yellow solid. ¹H NMR (400 MHz, CDCl₃) δ 1.32 (t, *J* = 7.1 Hz, 3H), 4.31 (q, *J* = 7.1 Hz, 2H), 7.73–7.76 (m, 1H), 8.29–8.33 (m, 1H), 8.78 (s, 1H), 9.33 (d, *J* = 8.6 Hz, 1H), 9.44 (d, *J* = 7.8 Hz, 1H), 9.96 (s, 1H). MS *m/z* = 246.08 (MH⁺).

General Procedure for the Preparation of Compounds 11b–h, j: 4-(2-Fluorophenyl)piperidine-4-carbonitrile (11c).

To a solution of *tert*-butyl bis(2-chloroethyl)carbamate (0.524 g, 2.16 mmol) and 2-fluorophenylacetone (0.292 g, 2.16 mmol) in DMSO (0.4 M, 5.4 mL) cooled to 18 °C was added sodium hydride (0.190 g, 4.76 mmol). The mixture was slowly warmed to room temperature, and after 1 h, was heated to 50 °C. After 17 h, the reaction was diluted with dichloromethane, washed 3 times with water, dried over sodium sulfate, filtered, and concentrated in vacuo. The residue was subjected to silica gel chromatography (0–25% ethyl acetate in hexanes) to provide *tert*-butyl-4-cyano-4-(2-fluorophenyl)piperidine-1-carboxylate as an orange oil.

A solution of *tert*-butyl-4-cyano-4-(2-fluorophenyl)piperidine-1-carboxylate (0.511 g, 1.68 mmol) in ethyl acetate (0.1 M, 16 mL) cooled to 0 °C was saturated with HCl(g) for 5 min. After 30 min, the reaction was concentrated in vacuo to provide the hydrogen chloride salt of 11c (0.408 g, >99%) as a white solid. MS *m/z* = 205.2 (MH⁺). ¹H NMR (400 MHz, CD₃OD) δ 2.41 (ddd, *J* = 3.8 Hz, 13.9 Hz, 13.9 Hz, 2H), 2.57 (m, 2H), 3.42 (ddd, *J* = 2.9 Hz, 13.5 Hz, 13.5 Hz, 2H), 3.63 (m, 2H), 7.24–7.34 (m, 2H), 7.50 (m, 1H), 7.57 (t, *J* = 1.6 Hz, 1H).

General Procedure for the Preparation of Compounds 11i, k–r: 4-Pyridin-2-ylpiperidine-4-carbonitrile (11i). To a solution of *tert*-butyl 4-cyanopiperidine-1-carboxylate (220 mg, 1.05 mmol) and 2-fluoropyridine (0.094 mL, 1.10 mmol) in THF (0.2 M, 5.2 mL) cooled to −78 °C under an atmosphere of nitrogen was added lithium bis(trimethylsilyl)amide (1.0 M in THF, 1.47 mL, 1.47 mmol). After 1 h, the reaction was warmed to room temperature. After an additional 1 h, the reaction was quenched with a saturated ammonium chloride solution, extracted 3 times with dichloromethane, dried over sodium sulfate, filtered, and concentrated in vacuo. The residue was subjected to

silica gel chromatography (0–20% ethyl acetate in hexanes) to provide *tert*-butyl 4-cyano-4-pyridin-2-ylpiperidine-1-carboxylate as a colorless oil.

A solution of *tert*-butyl 4-cyano-4-pyridin-2-ylpiperidine-1-carboxylate (3.11 g, 10.8 mmol) in ethyl acetate (0.2 M, 54 mL) and cooled to 0 °C was saturated with HCl(g) for 5 min. The reaction was warmed to rt and after 2 h, diluted with dichloromethane (100 mL), and neutralized with saturated aqueous sodium bicarbonate. The mixture was partitioned, and the aqueous layer was extracted 6 times with dichloromethane. The combined organic fractions were dried over sodium sulfate, filtered, and concentrated in vacuo to provide 11i (1.01 g, 99.0%) as a beige solid. MS *m/z* = 188.3 (MH⁺). ¹H NMR (400 MHz, CD₃OD) δ 2.26–2.39 (m, 4H), 3.20 (ddd, *J* = 3.2 Hz, 12.9 Hz, 12.9 Hz, 2H), 3.37–3.41 (dt, *J* = 2.9 Hz, 2.9 Hz, 13.4 Hz, 2H), 7.39 (m, 1H), 7.67 (d, *J* = 8.1 Hz, 1H), 7.90 (t, *J* = 7.8 Hz, 1H), 8.61 (d, *J* = 4.9 Hz, 1H).

General Procedure for the Preparation of Compounds 4a–v: 1-[(4-Cyano-4-pyridin-2-ylpiperidin-1-yl)methyl]-4-oxo-4H-quinolizine-3-carboxylic Acid (4i).

To a 10–20 mL Emrys process vial was added a solution of 8 (684 mg, 2.79 mmol), 11i (627 mg, 3.35 mmol), glacial acetic acid (0.96 mL, 16.7 mmol), and dichloroethane (0.68 M, 4.1 mL). The mixture was stirred vigorously, and resin-bound MP-cyanoborohydride (2.74 g, 5.58 mmol) was added. The reaction was irradiated in a Emrys Optimizer microwave to 120 °C for 30 min, then cooled to room temperature, filtered, and concentrated in vacuo. The residue was subjected to silica gel chromatography (55–75% ethyl acetate in hexanes) to provide ethyl 4-[(4-cyano-4-pyridin-2-ylpiperidin-1-yl)methyl]-1-oxo-1,8a-dihydronaphthalene-2-carboxylate as a yellow solid.

To a solution of ethyl 4-[(4-cyano-4-pyridin-2-ylpiperidin-1-yl)methyl]-1-oxo-1,8a-dihydronaphthalene-2-carboxylate (705 mg, 1.69 mmol) in a 2:1 mixture of THF/ethanol (0.2 M, 8.4 mL) was added aqueous sodium hydroxide NaOH (1.0 N, 1.78 mL, 1.78 mmol). The mixture was warmed to 60 °C for 16 h, cooled to room temperature, and concentrated in vacuo. The residue was subjected to purification via preparative reverse phase HPLC. The purified fractions were combined and concentrated in vacuo, then treated with aqueous sodium hydroxide (1.0 N, 2.74 mL, 2.74 mmol). After 1 h, the reaction was concentrated in vacuo. The residue was washed with cold water (5 mL), redissolved in methanol, and concentrated in vacuo to provide 4i (0.688 g, 80.0%) as a yellow solid. ¹H NMR (500 MHz, CD₃OD) δ 2.13 (d, *J* = 11.7 Hz, 2H), 2.23 (t, *J* = 12.7 Hz, 2H), 2.55 (t, *J* = 12.1 Hz, 2H), 3.09 (d, *J* = 12.2 Hz, 2H), 3.82 (s, 2H), 7.29 (t, *J* = 7.0 Hz, 1H), 7.32–7.36 (m, 1H), 7.62 (d, *J* = 8.0 Hz, 1H), 7.69 (t, *J* = 6.3 Hz, 1H), 7.85 (t, *J* = 7.8 Hz, 1H), 8.30 (s, 1H), 8.18 (d, *J* = 8.9 Hz, 1H), 8.55 (d, *J* = 3.9 Hz, 1H), 9.37 (d, *J* = 7.2 Hz, 1H). MS *m/z* = 389.16 (MH⁺).

Fluorometric Imaging Plate Reader (FLIPR) Assay. Chinese hamster ovary (CHO) cells under control of the nuclear factor of activated T cells (NFAT) promoter (CHONFAT) cells expressing M₁, M₂, M₃, M₄, M₅, rhesus M₁, dog M₁, mouse M₁, and rat M₁ (in CHOK1 from ATCC) receptors were plated (25,000 cells per well) in clear-bottomed, poly D-lysine-coated 384-well plates in growth medium by using a Labsystems (Chicago) Multidrop. The plated cells were grown overnight at 37 °C in the presence of 6% CO₂. The next day, the cells were washed with 3 × 100 μL assay buffer (Hanks' balanced salt solution containing 20 mM Hepes, 2.5 mM probenecid, and 0.1% BSA). The cells were incubated with 1 μM Fluo-4AM (Molecular Probes) for 1 h at 37 °C and 6% CO₂. The extracellular dye was removed by washing as described above. Ca²⁺ flux was measured by using a FLIPR₃₈₄ fluorometric imaging plate reader (Molecular Devices). Compounds were serially diluted in 100% DMSO and then diluted in assay buffer to a 3 × stock at 2% DMSO. This stock was then applied to the cells for a final DMSO concentration of 0.67%. For potency determination, the cells were preincubated with various concentrations of compound for 4 min and then stimulated for 4 min with an EC₂₀ concentration of agonist (i.e., ACh) for potentiation measurements.

Fold Potentiation Assay. CHO_{NFAT} cells expressing human mAChR 1 receptor were plated (25,000 cells per well) in clear-bottomed, poly D-lysine-coated 384-well plates in growth medium by using a Labsystems (Chicago) Multidrop. The plated cells were grown overnight at 37 °C in the presence of 6% CO₂. The next day, the cells were washed with 3 × 100 μ L assay buffer (Hanks' balanced salt solution containing 20 mM Hepes, 2.5 mM probenecid, and 0.1% BSA). The cells were incubated with 1 μ M Fluo-4AM (Molecular Probes) for 1 h at 37 °C and 6% CO₂. The extracellular dye was removed by washing as described above. Ca²⁺ flux was measured by using a FLIPR₃₈₄ fluorometric imaging plate reader (Molecular Devices). Compounds were dissolved in 100% DMSO and then diluted in assay buffer to a 3 × stock at 2% DMSO. This stock was then applied to the cells for a final DMSO concentration of 0.67%. For the fold potentiation measurements, the cells were preincubated with various concentrations of compound for 4 min and then stimulated for 4 min with a serially diluted agonist (i.e., ACh).

Transepithelial Transport Assay of P-gp. Transepithelial transport study was conducted as described²² with minor modifications. The cells were maintained in M199 media supplemented with 10% FBS. The cells at a density of 5 × 10⁴ cells/mL were plated onto a 96-well filter with 150 μ L/well (porous size 3.0- μ m, 0.11 cm² surface areas; Millipore Corp., Bedford, MA). Cells were supplemented with fresh media on the third day and used for the transport studies on the fourth day after plating. The concentrations of all test compounds were at 5 μ M unless otherwise indicated. Verapamil at 1 μ M concentration was used as a marker Pgp substrate for a positive control (Sigma-Aldrich (St. Louis, MO)). Hanks' balanced salt solution (HBSS, Gibco-Invitrogen Corporation, Carlsbad, CA), serum/protein free medium, was used through the experiments to eliminate any differences in protein binding among the compounds tested. Before the addition of testing compounds, the media were first replaced with HBSS media containing 1 mM HEPES to equilibrate cells into experimental conditions for 30 min. The transport experiment was then initiated by replacing the medium in each compartment with 150 μ L of fresh HBSS with or without the test compound. After 3 h of incubation, 100 μ L aliquots were taken from the opposite compartment as receiver samples and from the loading compartment as donor samples. The samples of the radioactive compounds were placed in scintillation vials containing 5 mL of scintillation cocktail, and total radioactivity was measured by a liquid scintillation counter. The appearance of radioactivity in the opposite compartment was presented as a fraction of the total radioactivity added at the beginning of the experiment. Directional transport was measured in triplicate and presented as the mean \pm SD. The samples of nonradio-labeled test compounds were analyzed by LC/MS/MS.

Contextual Fear Conditioning. On day one, 10-week-old experimentally naïve male B6SJL mice (n = 12–16/group) were dosed IP with test compound in 5% betacyclodextrin and/or 0.3 mg/kg scopolamine in 0.9% saline 30 min before placement into a chamber (MED-VFC-M, Med Associates) for 2 min before 2 tone-footshock pairings (3 kHz, 85 dB tone for 30 s coterminated with a 0.5 mA, 1 s shock) 2 min apart. Mice were removed to their home cage 30 s after the last pairing. Twenty-four hours later, mice were placed into the same chamber, and freezing was measured by Video Freeze (Med Associates).

AUTHOR INFORMATION

Corresponding Author

*Department of Medicinal Chemistry, Merck Research Laboratories, WP14-3, P.O. Box 4, West Point, PA 19486. Tel: (215) 652-5147. Fax: (215) 652-3971. E-mail: scott_d_kuduk@merck.com.

ACKNOWLEDGMENT

We thank Dr. Deanne Rudd, James Marr, and Joan Ellis for pharmacokinetic analysis, Kim Michel and Anne Taylor for

animal dosing, Matt Zrada for protein binding studies, and Keith Jones, Valerie Kuzmick-Graufelds, Denise Bickel, and Maryann Bruno for support with CFC studies.

ABBREVIATIONS USED

CNS, central nervous system; IP, inflection point; PB, protein binding; P-gp, P-glycoprotein; SAR, structure–activity relationship; HTS, high throughput screening; MDR, multidrug resistance; AD, Alzheimer's disease; ACh, acetylcholine; FLIPR, fluorometric imaging plate reader; HBSS, Hank's balanced salt solution; NADPH, nicotinamide adenine dinucleotide phosphate; UDPGA, uridine diphosphate α -D-glucuronic acid; UGT, uridine glucuronosyltransferase; CHONFAT, chinese hamster ovary (CHO) cells under control of the nuclear factor of activated T cells (NFAT) promoter

REFERENCES

- (1) Geula, C. Abnormalities of neural circuitry in Alzheimer's disease: hippocampus and cortical innervation. *Neurology* **1998**, *51*, S18–29.
- (2) Bonner, T. I. The molecular basis of muscarinic receptor diversity. *Trends Neurosci.* **1989**, *12*, 148–151.
- (3) Bonner, T. I. New subtypes of muscarinic acetylcholine receptors. *Trends Pharmacol. Sci.* **1989**, 11–15.
- (4) Langmead, C. J.; Watson, J.; Reavill, C. Muscarinic acetylcholine receptors as CNS drug targets. *Pharmacol. Ther.* **2008**, *117*, 232–243.
- (5) Bodick, N. C.; Offen, W. W.; Levey, A. I.; Cutler, N. R.; Gauthier, S. G.; Satlin, A.; Shannon, H. E.; Tollefson, G. D.; Rasmussen, K.; Bymaster, F. P.; Hurley, D. J.; Potter, W. Z.; Paul, S. M. Effects of Xanomeline, a selective muscarinic receptor agonist, on cognitive function and behavioral symptoms in Alzheimer. Disease. *Arch. Neurol.* **1997**, *54*, 465–473.
- (6) Greenlee, W.; Clader, J.; Asbersom, T.; McCombie, S.; Ford, J.; Guzik, H.; Kozlowski, J.; Li, S.; Liu, C.; Lowe, D.; Vice, S.; Zhao, H.; Zhou, G.; Billard, W.; Binch, H.; Crosby, R.; Duffy, R.; Lachowicz, J.; Coffin, V.; Watkins, R.; Ruperto, V.; Strader, C.; Taylor, L.; Cox, K. Muscarinic agonists and antagonists in the treatment of Alzheimer's disease. *Il Farmaco* **2001**, *56*, 247–250.
- (7) Conn, P. J.; Christopoulos, A.; Lindsley, C. W. Allosteric modulators of GPCRs: a novel approach for the treatment of CNS disorders. *Nat. Rev. Drug Discovery* **2009**, *8*, 41–54.
- (8) Spalding, T. A.; Trotter, C.; Skjaerbaek, N.; Messier, T. L.; Currier, E. A.; Burstein, E. S.; Li, D.; Hacksell, U.; Brann, M. R. Discovery of an ectopic activation site on the M₁ muscarinic receptor. *Mol. Pharmacol.* **2002**, *61*, 1297–1302.
- (9) Jones, C. K.; Brady, A. E.; Davis, A. A.; Xiang, Z.; Bubser, M.; Tantouwy, N.; Kane, A. S.; Bridges, T. M.; Kennedy, J. P.; Bradley, S. R.; Peterson, T. E.; Ansari, M. S.; Baldwin, R. M.; Kessler, R. M.; Deutch, A. Y.; Lah, J. J.; Levey, A. I.; Lindsley, C. W.; Conn, P. J. Novel selective allosteric activator of the M₁ muscarinic acetylcholine receptor regulates amyloid processing and produces antipsychotic-like activity in rats. *J. Neurosci.* **2008**, *41*, 10422–10433.
- (10) Conn, P. J.; Jones, C. K.; Lindsley, C. W. Subtype-selective allosteric modulators of the muscarinic receptors for the treatment of CNS disorders. *Trends Pharmacol. Sci.* **2009**, *30*, 148–155.
- (11) Ma, L.; Seager, M.; Wittmann, M.; Jacobsen, M.; Bickel, D.; Burno, M.; Jones, K.; Kuzmick-Graufelds, V.; Xu, G.; Pearson, M.; McCampbell, A.; Gaspar, R.; Shughue, P.; Danziger, A.; Regan, C.; Flick, R.; Pascarella, D.; Garson, S.; Doran, S.; Kreatsoulas, C.; Veng, L.; Lindsley, C.; Shipe, W.; Kuduk, S. D.; Sur, C.; Kinney, G.; Seabrook, G.; Ray, W. J. Selective activation of the M₁ muscarinic acetylcholine receptor achieved by allosteric potentiation. *Proc. Natl. Acad. Sci. U.S.A.* **2009**, *106*, 15950–15955.
- (12) Shirey, J. K.; Brady, A. E.; Jones, P. J.; Davis, A. A.; Bridges, T. M.; Kennedy, J. P.; Jadhav, S. B.; Menon, U. N.; Xiang, Z.; Watson,

M. L.; Christian, E. P.; Doherty, J. J.; Quirk, M. C.; Snyder, D. H.; Lah, J. J.; Levey, A. I.; Nicolle, M. M.; Lindsley, C. W.; Conn, P. J. A selective allosteric potentiator of the M₁ muscarinic acetylcholine receptor increases activity of medial prefrontal cortical neurons and restores impairments in reversal learning. *J. Neurosci.* **2009**, *45*, 14271–14286.

(13) Kuduk, S. D.; Di Marco, C. N.; Chang, R. K.; Ray, W. J.; Ma, L.; Wittmann, M.; Seager, M.; Koeplinger, K. A.; Thompson, C. D.; Hartman, G. D.; Bilodeau, M. T. Heterocyclic fused pyridone carboxylic acid M₁ positive allosteric modulators. *Bioorg. Med. Chem. Lett.* **2010**, *20*, 2533–2537.

(14) Kuduk, S. D.; DiPardo, R. M.; Beshore, D. C.; Ray, W. J.; Ma, L.; Wittmann, M.; Seager, M.; Koeplinger, K. A.; Thompson, C. D.; Hartman, G. D.; Bilodeau, M. T. Hydroxy cycloalkyl fused pyridone carboxylic acid M₁ positive allosteric modulators. *Bioorg. Med. Chem. Lett.* **2010**, *20*, 2538–2541.

(15) Kuduk, S. D.; Chang, R. K.; Di Marco, C. N.; Ray, W. J.; Ma, L.; Wittmann, M.; Seager, M. A.; Koeplinger, K. A.; Thompson, C. D.; Hartman, G. D.; Bilodeau, M. T. Identification of quinolizidinone carboxylic acids as CNS penetrant, selective M₁ allosteric muscarinic receptor modulators. *ACS Med. Chem. Lett.* **2010**, *1*, 263–267.

(16) Kuduk, S. D.; Chang, R. K.; Di Marco, C. N.; Ray, W. J.; Ma, L.; Wittmann, M.; Seager, M.; Koeplinger, K. A.; Thompson, C. D.; Hartman, G. D.; Bilodeau, M. T. Quinolizidinone carboxylic acid selective M₁ allosteric modulators: SAR in the piperidine series. *Bioorg. Med. Chem. Lett.* **2011**, *21*, 1710–1715.

(17) Kuduk, S. D.; Chang, R. K. Quinolizidinone M₁ Receptor Positive Allosteric Modulators. WO 2009051715, 2009.

(18) Komatsu, H.; Iwasawa, N.; Citterio, D.; Suzuki, Y.; Kubota, T.; Tokuno, K.; Kitamura, Y.; Oka, K.; Suzuki, K. Design and synthesis of highly sensitive and selective fluorescein-derived magnesium fluorescent probes and application to intracellular 3D Mg²⁺ imaging. *J. Am. Chem. Soc.* **2004**, *126*, 16353–16360.

(19) Chang, R. K.; Di Marco, C. N.; Pitts, D. R.; Greshock, T. J.; Kuduk, S. D. Preparation of 4-heteroaryl-4-cyanopiperidines via S_NAr substitution reactions. *Tetrahedron Lett.* **2009**, *50*, 6303–6306.

(20) Maurer, T. S.; DeBartolo, D. B.; Tess, D. A.; Scott, D. O. Relationship between exposure and nonspecific binding of thirty-three central nervous system drugs in mice. *Drug Metab. Dispos.* **2005**, *33*, 175–181.

(21) Kim, J. J.; Fasnow, M. S. Modality-specific retrograde amnesia of fear. *Science* **1992**, *256*, 675–677.

(22) Yamazaki, M.; Neway, W. E.; Ohe, T.; Chen, I.; Rowe, J. F.; Hochman, J. H.; Chiba, M.; Lin, J. H. In vitro substrate identification studies for P-glycoprotein-mediated transport: species difference and predictability of in vivo results. *J. Pharmacol. Exp. Ther.* **2001**, *296*, 723–735.